Journal of Solid State Chemistry 182 (2009) 1359–1364

Contents lists available at ScienceDirect

Journal of Solid State Chemistry

journal homepage: www.elsevier.com/locate/jssc

Chemical interaction in the B–BN system at high pressures and temperatures. Synthesis of novel boron subnitrides

Vladimir L. Solozhenko *, Oleksandr O. Kurakevych

LPMTM-CNRS, Université Paris Nord, 99, av. J.-B. Clement, 93430 Villetaneuse, France

ARTICLE INFO

Article history:
Received 2 December 2008
Received in revised form
16 February 2009
Accepted 4 March 2009
Available online 14 March 2009

Keywords:
Boron-rich compounds
Boron subnitride
High pressure
High temperature
X-ray diffraction
In situ

ABSTRACT

Chemical interaction and phase transformations in the B–BN system have been *in situ* studied by X-ray diffraction with synchrotron radiation at pressures up to 5.3 GPa and temperatures up to 2800 K using multianvil press. New rhombohedral boron subnitride $B_{13}N_2$ has been synthesized by crystallization from the B–BN melt at 5 GPa. The structure of $B_{13}N_2$ belongs to the *R*-3*m* space group ($a = 5.4455(2)$ Å, $c = 12.2649(9)$ Å) and represents a new structural type. The subnitride is an individual compound and not a solid solution, in contrast to boron carbide. Besides, the formation of two other boron-rich B–N phases denoted as "B_6N" and "$B_{50}N_2$" has been observed. Their structures seem to be much more sophisticated and have not been even resolved to present time.

1. Introduction

Boron-rich solids give a rise to a large group of refractory compounds with unique crystal structures and interesting physical and chemical properties related to the strongly covalent and electron-deficiency character of their chemical bonds [1,2]. Phases with structures related to α-rhombohedral boron (α-rh boron) include boron carbide B_4C and boron suboxide B_6O, that combine lightness, strength, high hardness and wear resistance, chemical inertness, high melting point as well as high cross-section for neutron absorption [3–5]. The high pressure synthesis of new phases with boron-like structures may lead to novel materials with advanced properties exceeding those of B_4C and B_6O. For example, in literature there are some speculations on the probable metallic conductivity of the B_6N phase [6].

The existence of boron subnitride B_6N was first suggested by Condon et al. [7] in the work devoted to the kinetics of the boron reaction with nitrogen. Later, the synthesis of the B–N films containing subnitride "B_4N" was reported by Saitoh et al. [8]; however, neither structure nor composition of the synthesized compounds have been established [7,8]. Hubert et al. [9] reported the high-pressure solid-state synthesis of boron subnitride "$B_6N_{0.92}$" by reacting amorphous boron and hexagonal graphite-like boron nitride (hBN) at 7.5 GPa and ~2000 K. Based on the EELS data, the authors claimed the $B_6N_{0.92}$ composition [9]; however, according to our recent results [10], the diffraction pattern reported in [9] cannot belong to any B_6O-like or B_4C-like structure.

In the present work, we have *in situ* studied the chemical interaction and phase relations in the B–BN system at pressures up to 5 GPa and temperatures up to 2800 K. The new boron subnitride $B_{13}N_2$ has been synthesized by quenching of the B–BN melt at 5 GPa and characterized by X-ray powder diffraction, Raman spectroscopy, transmission electron microscopy (TEM) and electron energy loss spectroscopy (EELS).

2. Experimental

A powder of β-rh boron [11] or amorphous boron (claimed purity 99.99%, Alfa Aesar) has been mixed with hBN (claimed purity 99.8%, Johnson Matthey GmbH) in several B:BN molar ratios (from 21:1 to 2:1). A starting mixture has been pressed into a pellet, enclosed in a hBN capsule and placed inside a graphite resistance furnace of the high-pressure cell assembly. The high pressure–high temperature syntheses have been carried out using a multianvil X-ray system MAX80 at beamline F2.1, HASYLAB-DESY. The experimental set up has been described elsewhere [12]. Energy-dispersive data has been collected on a Canberra solid state Ge-detector with fixed Bragg angle $2\theta = 9.12(4)^\circ$ using a white beam collimated to $60 \times 100\,\mu m^2$ (vertical by horizontal) and the detector optics with 2θ acceptance angle of 0.005°, which

* Corresponding author. Fax: +33 149403938.
E-mail addresses: vls@lpmtm.univ-paris13.fr (V.L. Solozhenko), kura@lpmtm.univ-paris13.fr (O.O. Kurakevych).

0022-4596/$ - see front matter © 2009 Elsevier Inc. All rights reserved.
doi:10.1016/j.jssc.2009.03.003

ensures a high resolution of the observed diffraction patterns. With the storage ring operating at 4.44 GeV and 150 ± 50 mA, diffraction patterns have been collected for 1–2 min in real time. The detector has been calibrated using the K_α and K_β fluorescence lines of Cu, Rb, Mo, Ag, Ba, and Tb. The sample pressure has been determined from the lattice constants of highly ordered hBN using corresponding equation of state [13].

Samples have been gradually compressed to required pressure at ambient temperature, and then diffraction patterns have been collected at the stepwise (~50 K) temperature increase. Pressures at different temperatures have been found from the *p-V-T* data on highly ordered ($P_3 = 0.98 \pm 0.02$) graphite-like hexagonal boron nitride using the thermoelastic equation of state suggested in [12]. The sample temperature up to 2200 K has been measured by a W3%Re–W25%Re thermocouple. Above 2200 K the power–temperature calibration curve has been linearly extrapolated to the high-temperature region (up to 2800 K). After heating, the samples have been quenched by the switching off the power (the initial cooling rate was about 400–500 K/s).

The recovered samples have been analyzed by powder X-ray diffraction using G3000 TEXT (Inel) and D5000 (Siemens) powder X-ray diffractometers in a Bragg–Brentano geometry employing Cu$K\alpha$ radiation. The alignment of goniometers and calibration of linear detector have been performed using high purity silicon ($a = 5.431066$ Å) and the standard sample of LaB_6 ($a = 4.15695$ Å). Unit cell parameters have been derived from the LeBail profile refinement procedure [14] performed using the GSAS computer program [15]. Highly ordered hBN has been used as an internal standard.

Microstructure and phase composition of the samples have been studied by TEM-EELS using a JEM 2010HR (JEOL) transmission electron microscope equipped with a GIF2000 (GATAN) parallel electron energy loss spectrometer. ELLS spectra have been collected from the regions less than $10 \times 10\,nm^2$, i.e. the established composition corresponds to the individual crystalline grains whose structure can be recognized by selected area electron diffraction.

The Raman scattering measurements have been performed at 300 K using a Dilor XY system with the 514.5 nm Ar^+ ion laser as excitation source. The scattered light has been collected in the backscattering geometry using a CCD detector. The spectrometer has been calibrated using the Γ_{25} phonon of Si (*Fd*-3*m*). The incident laser power has been 50–75 mW. No modifications in the Raman peaks have been observed within the laser power range used in our experiments.

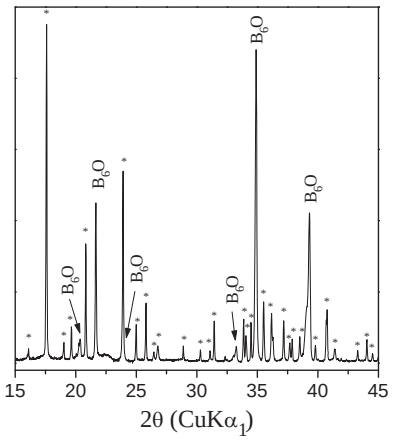

Fig. 1. Powder diffraction pattern of a sample of amorphous boron quenched from 2570 K and 5.3 GPa. The stars represent the diffraction lines of β-rh boron.

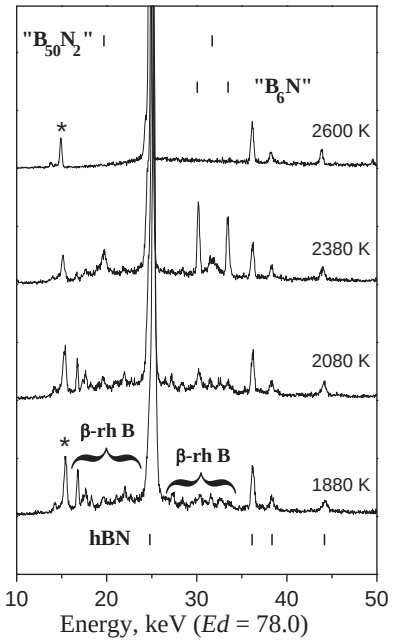

Fig. 2. Sequence of energy-dispersive diffraction patterns of mixture of β-rh boron and hBN (molar ratio 5:1) taken *in situ* at 5.0 GPa and different temperatures. Above 2080 K two diffraction lines corresponding to the "B_6N" phase arise; at 2380 K the lines of *β*-rh boron are almost disappeared due to the melting, and finally at 2600 K, the "B_6N" melts.

3. Results and discussion

Our preliminary experiments have revealed that the oxygen contamination plays an important role when amorphous boron is used as starting material for reaction with boron nitride. Fig. 1 shows a powder diffraction pattern of amorphous boron quenched from 2570 K and 5.3 GPa. Intensive lines of B_6O together with the reflections of β-rh boron are clearly seen which is indicative of the partial oxidation of amorphous boron and its transformation into thermodynamically stable β-rh boron.

X-ray powder diffraction patterns of all B-BN samples containing amorphous boron (molar ratios B:BN from 21:1 to 5:1) quenched from 2300 to 2600 K at ~5 GPa show lines of a B_6O-like phase. The remarkable variation of the lattice parameters, within 0.07 Å for *a*-parameter and 0.05 Å for *c*-parameter, allows one to conclude that the synthesized phase is the $B_6(N_{1-x}O_x)_{1-y}$ solid solution. Most probably, at high temperatures amorphous boron has been oxidized to B_2O_3 by the adsorbed water and/or oxygen [16]; and the molten boron oxide interacted with boron and hBN resulting in the formation of $B_6(N_{1-x}O_x)_{1-y}$.

In contrast to amorphous boron, in high-pressure cell β-rh boron is stable to oxidation up to its melting point, and, therefore, the oxygen impurities in resulting samples can be drastically reduced. That is why, to synthesize an oxygen-free boron subnitride, we have used β-rh boron as starting material.

The typical sequence of the powder diffraction patterns taken *in situ* during the heating of the mixture of β-rh boron and hBN (molar ratios B:BN from 6:1 to 4:1) at 5 GPa is presented in Fig. 2. At temperatures above 2080 K, two diffraction lines appear that could be interpreted as those of a B_6O-like phase (herein and after called "B_6N"). In the 2100–2300 K range this phase may be quenched down to ambient conditions; and its powder diffraction pattern (Fig. 3) shows two fine well-formed lines close to the 1 0 4, 0 2 1 and, for some samples, 1 1 0 reflections of the B_6O-like lattice, while the expected 1 0 1, 0 0 3 and 0 1 2 reflections are very weak

(about 10 times less intensive than expected for the phases with structure related to α-rh boron). Similar powder diffraction patterns have been reported by Hubert et al. [9] for the phase "$B_6N_{0.92}$" in the quenched samples of the mixture of amorphous boron with hBN from 7 GPa and 2000 K. According to our *in situ* observations, in the case of amorphous boron as a starting material, at 5 GPa the diffraction lines of "B_6N" appear already at about 1600 K. The structure of "B_6N" phase has not been resolved so far and should be related to a new boron modification stabilized by nitrogen and/or oxygen contamination [10].

The heating of the B–BN mixtures above 2380 K is accompanied by the disappearance of the β-rh boron lines due to the boron melting (Fig. 2). The quenching of the samples having the B_6N and B_5N compositions from 2400 to 2600 K leads to the formation of the well-crystallized rhombohedral boron subnitride phase with structure related to α-rh B and general stoichiometry $B_{12+x}N_{2+y}$. X-ray diffraction patterns of the well-powdered quenched samples (Fig. 4) shows the lines corresponding to a B_6O-like lattice, namely, 101, 003, 012, 110, 104, 0021, 024, 303, 018, 125, 220, 131, 223, 217, 119 and 134. The lattice parameters have been found to be $a = 5.4455(2)$ Å and $c = 12.2649(9)$ Å (trigonal syngony, hexagonal axis, space group *R*-3*m*), which are intermediate between those of boron suboxide B_6O ($a = 5.367(2)$ Å, $c = 12.325(3)$ Å according to JCPDS no. 87–1143) and boron carbide $B_{13}C_2$ ($a = 5.633(8)$ Å, $c = 12.164(2)$ Å according to [17]), see Fig. 5a. The variation of lattice parameters of the as-synthesized $B_{12+x}N_{2+y}$ subnitride in all our experiments has not exceeded ±0.002 Å for *a*-parameter and ±0.001 Å for *c*-parameter, which allows us to conclude that the resulting phase is an individual subnitride and not a solid solution.

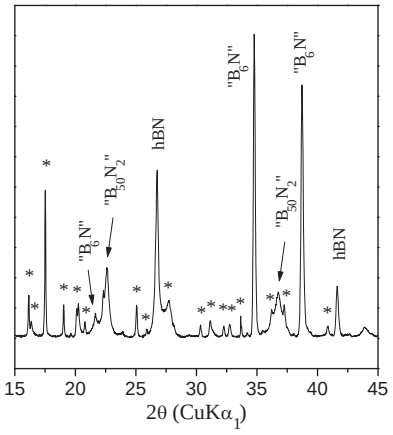

Fig. 3. Powder diffraction pattern of a mixture of β-rh boron and hBN (the molar ratio 5:1) quenched from 2300 K and 4.7 GPa. The stars represent the diffraction lines of β-rh boron.

The structure of $B_{12+x}N_{2+y}$ has been determined by Rietveld refinement of powder diffraction data collected at ambient conditions (Fig. 6, Table 1). The satisfactory refinement has been achieved only in the case of the *R*-3*m* starting unit cell containing two symmetrically independent boron atoms of the 18*h* Wickoff position, one independent nitrogen atom of 6*c* position and one boron atom of 3*b* position. The phase has a structure similar in some respect to those of α-rh B [18], $B_{4+z}C_{1-z}$ [17,19], and B_6O [19,20]. The $B_{12+x}N_{2+y}$ phase features distorted B_{12} icosahedra linked by N–B–N chains, giving rise to a three-dimensional framework. The similarity is greatest to $B_{4+z}C_{1-z}$, which has the same unit cell, space group, and atom sites as the subnitride. The site occupancies of the atoms of each crystallographic type are close to unit, so the synthesized phase has the $B_{13}N_2$ stoichiometry.

According to the TEM observations, the synthesized phase occurs as aggregates with clearly visible (average size 200 nm) grains. The morphology typical for trigonal crystals may be easily recognized. From the EELS data the stoichiometry of $B_{12+x}N_{2+y}$ phase has been determined to be $B_{6\pm1}N$, which is in good agreement with $B_{13}N_2$ composition, established by Rietveld refinement of X-ray powder diffraction patterns. The three strongest diffraction rings of the selected area electron diffraction (SAED) patterns, i.e. 003, 104, and 021 have been used to recognize the $B_{13}N_2$ particles. According to the data of TEM-EELS, $B_{13}N_2$ phase contain only nitrogen and boron. No detectable amounts of oxygen or carbon have been observed.

In some experiments, reddish microcrystals of pinacoidal habit with size up to 50 μm have been observed after quenching on the phase boundary between a B–BN (or boron) sample and hBN capsule (Fig. 7). According to selected-area electron diffraction, they are the single crystals, if not twins, of $B_{13}N_2$.

The Raman spectra of the $B_{13}N_2$ microcrystals (Fig. 8) are similar to those of B_6O and B_4C [19]. One can observe the inter-icosahedral modes above 950 cm^{-1}, the intra-icosahedral modes between 400 and 950 cm^{-1} and the modes with wavenumber less then 400 cm^{-1} that are, most probably, librational (involving rotation of icosahedra, etc.). All the lines above 600 cm^{-1} are

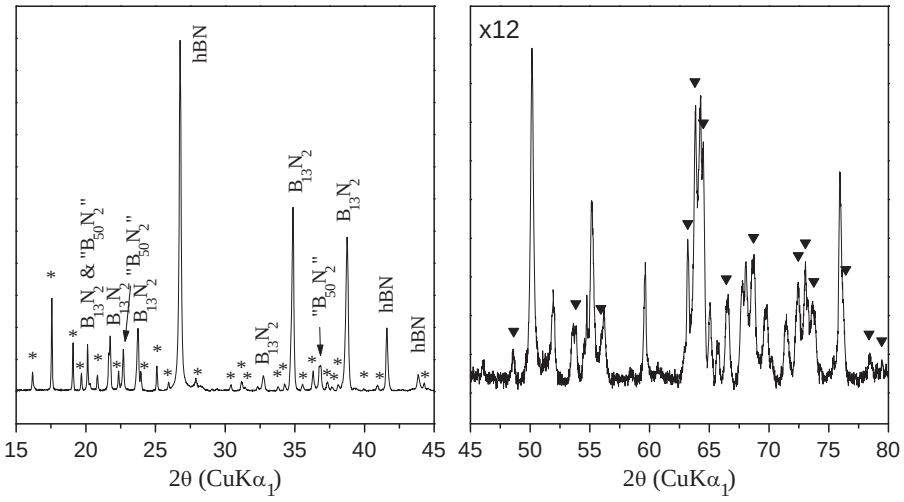

Fig. 4. Powder diffraction pattern of a mixture of β-rh boron and hBN (the molar B:BN ratio 5:1) quenched from 2600 K and 4.9 GPa. The stars represent the diffraction lines of β-rh boron, while the triangles on the right figure correspond to the $B_{13}N_2$ lines.

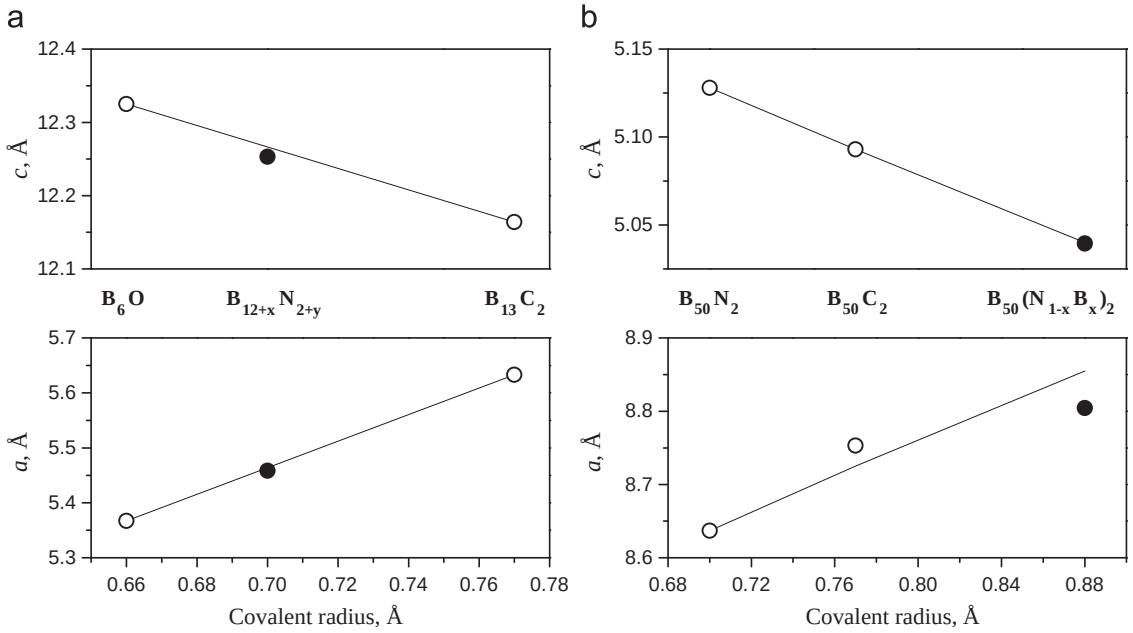

Fig. 5. Dependence of the lattice parameters of phases with structures related to α-rh boron (B_6O, $B_{13}N_2$ and B_4C) (a) and to I-t boron ($B_{50}N_2$, $B_{50}C_2$, and $B_{50}(N_{1-x}B_x)_2$) (b) on the covalent radii of the interstitial atoms.

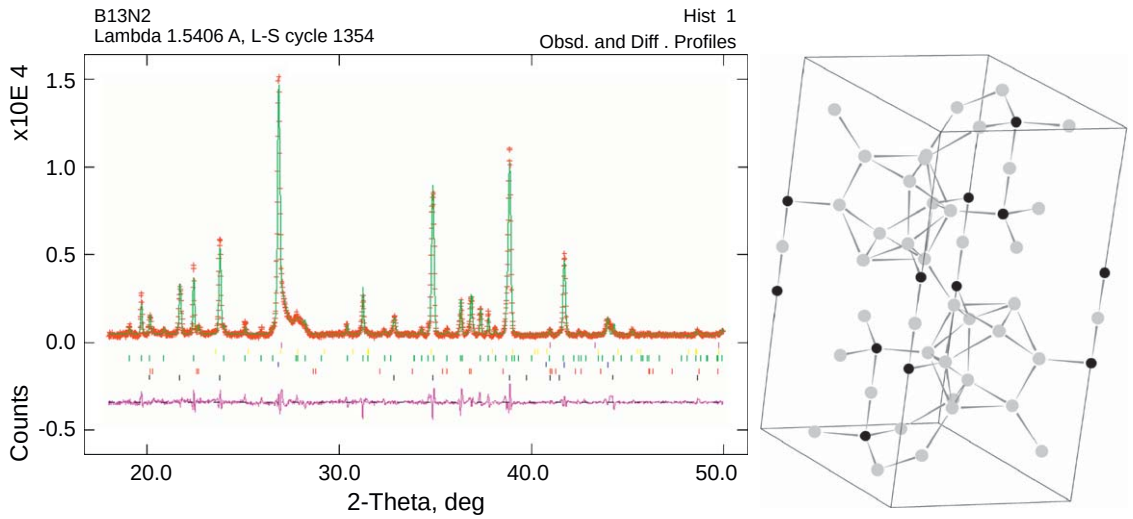

Fig. 6. Rietveld analysis and structure of rhombohedral boron subnitride $B_{13}N_2$. Since the $B_{13}N_2$ phase crystallizes by peritectic reaction together with β-rh boron, "$B_{50}N_2$" and hBN, all four phases have been used for the Rietveld full profile refinement of the X-ray powder diffraction pattern of $B_{13}N_2$.

Table 1
Results of the Rietveld refinement of atomic coordinates and fractions.

No.	Atom	Wickers index	*x*	*y*	*z*	Fraction
1	B	18*h*	**0.1725(14)**	−0.1725	**0.0371(13)**	1
2	B	18*h*	**0.1198(7)**	−0.1198	**0.8834(8)**	1
3	N	6*c*	0	0	**0.3744(13)**	1
4	B	3*b*	0	0	0.5000	**1.00(2)**

The refined parameters are given in bold. *R*-3*m*, $a = 5.4455(2)$ Å, $c = 12.2649(9)$ Å, $Z = 3$, $D = 2.666\ g\,cm^{-3}$, no. of reflections: 11, $R_F^2 = 0.02645$.

usually attributed to vibrations of the atoms of boron-rich icosahedra [14]. The fine feature just below 500 cm^{-1} corresponds to the symmetric stretching of the N–B–N chains and the narrow line just above 500 cm^{-1}, to the motion of icosahedron about nitrogen atom [19].

Over the whole *p-T* range under study $B_{13}N_2$ crystallizes in mixture with β-rh boron, a phase similar to boron-rich tetragonal subnitride $B_{50}N_2$ ("$B_{50}N_2$", a phase with structure of hypothetical I-t boron) [21] and hBN (Fig. 4). The amount of the $B_{13}N_2$ phase in relation to $B_{50}N_2$-like phase increases with a higher BN content in the starting mixture; however, synthesis of single-phase $B_{13}N_2$ seems to be impossible because its formation at 5 GPa occurs according to the $L + hBN \rightleftarrows B_{13}N_2$ peritectic reaction.

The powder diffraction pattern of the well-crystallized "$B_{50}N_2$" phase is very similar to that of $B_{50}N_2$ [21], but not the same. Reflections 200, 101, 111, 002, 311, 321, 411, 312, 431, and 600 are present; however, the 110 line is absent. The lattice parameters of "$B_{50}N_2$" have been found to be $a = 8.8044(7)$ Å, $c = 5.0395(6)$ Å (*P*4*nnm* or *P*-4*n* space group), which remarkably differ from those of boron subcarbide $B_{50}C_2$ ($a = 8.753$ Å, $c = 5.093$ Å) and boron subnitride $B_{50}N_2$ ($a = 8.634$ Å, $c = 5.128$ Å)

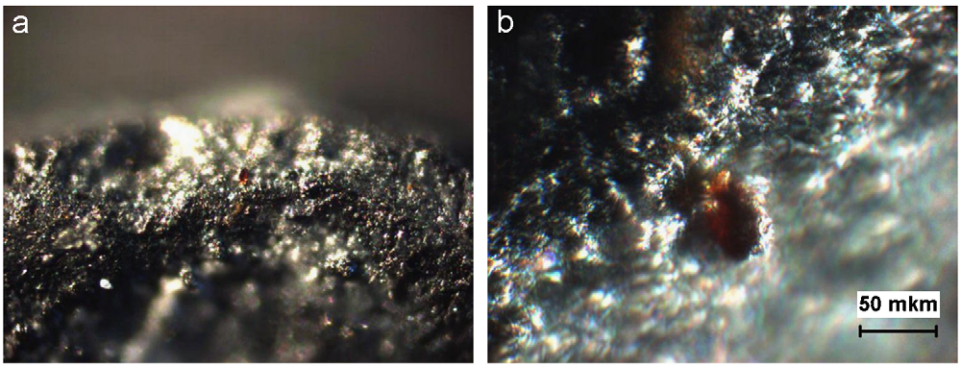

Fig. 7. Optical microscope pictures of $B_{13}N_2$ microcrystals with size of about 50 μm grown on the boundary between liquid boron and hBN at 2670 K and 5.3 GPa (*a*: × 10, *b*: × 50).

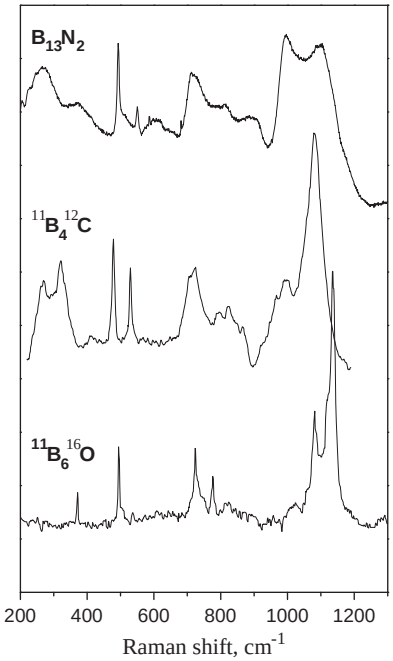

Fig. 8. Raman spectrum of the $B_{13}N_2$ microcrystal grown on the boundary between liquid boron and hBN at 2670 K and 5.3 GPa. The B_4C and B_6O Raman spectra[15] are shown for comparison.

[21]. The *a*-parameter of the "$B_{50}N_2$" phase observed in our experiments is higher, while *c*-parameter is smaller (Fig. 5b); that is indicative of a higher atomic radius of the atoms linking the icosahedra in comparison with carbon and nitrogen. These atoms are, most probably, the B atoms that substitute a number of N atoms in the $B_{50}N_2$ lattice. According to our crystallographic simulations using PowderCell program [22], the substitution of nitrogen for boron in the $B_{50}N_2$ unit cell [21] leads to the disappearance of the 110 line. Since the formation of "$B_{50}N_2$" has been never observed during the remelting of pure boron (α-rh or β-rh) at the same *p-T* conditions, one may suggest that the synthesized phase is nitrogen-doped I-t boron, i.e. $B_{50}(N_{1-x}B_x)_2$ whose structure has been stabilized at high pressure.

4. Conclusion

New rhombohedral boron subnitride $B_{13}N_2$ has been synthesized from the mixture of β-rh boron and hexagonal graphite-like boron nitride at ~5 GPa and 2300–2600 K. $B_{13}N_2$ crystallizes from the B–BN melt according to the peritectic reaction and has a structure related to α-rh boron. Raman spectra are in a good agreement with established structure and similar to the spectra of other boron-rich compounds. At the same time, a boron-rich phase with unknown structural type forms at ~5 GPa and 2100–2300 K, i.e. at temperatures below the B–BN melt formation. Besides, in the samples synthesized at ~5 GPa and temperatures higher than 2100 K a new nitrogen-boron phase with I-t boron structure has been observed, that is, most probably, nitrogen-doped I-t boron, whose structure has been stabilized at high pressure. Rhombohedral subnitride is predicted to be superhard [23,24] and may have metallic conductivity [6]. Unfortunately, the $B_{13}N_2$ crystallization by peritectic reaction in the studied *p-T* range did not allow us to study such properties so far.

Acknowledgments

The authors thank Dr. C. Lathe for assistance in high-pressure experiments and Prof. Dr. V.Z. Turkevich for valuable discussions. Experiments at HASYLAB-DESY have been supported by the GFZ-Potsdam under the MAX80 program. This work was financially supported by Agence Nationale de la Recherche (Grant ANR-05-BLAN-0141) and by the North Atlantic Treaty Organization (CLG#981851).

References

[1] T. Lundström, Y.G. Andreev, Mater. Sci. Eng. A 209 (1996) 16–22.
[2] A.R. Oganov, J. Chen, C. Gatti, Y. Ma, Y. Ma, C.W. Glass, Z. Liu, T. Yu, O.O. Kurakevych, V.L. Solozhenko, Nature 457 (2009) 863–867.
[3] D. Emin, in: Materials Research Society Symposia Proceedings, MRS, vol. 97, Pittsburgh, 1987.
[4] A.R. Badzian, Appl. Phys. Lett. 53 (1988) 2495–2497.
[5] H.F. Rizzo, W.C. Simmons, H.O. Beilstein, J. Electrochem. Soc. 109 (1962) 1079–1082.
[6] P.F. McMillan, Nat. Mater. 1 (2002) 19–25.
[7] J.B. Condon, C.E. Holcombe, D.H. Johnson, L.M. Steckel, Inorg. Chem. 15 (1976) 2173–2179.
[8] H. Saitoh, K. Yoshida, W.A. Yarbrough, J. Mater. Res. 8 (1993) 8–11.
[9] H. Hubert, L.A.J. Garvie, P.R. Buseck, W.T. Petuskey, P.F. McMillan, J. Solid State Chem. 133 (1998) 356–364.
[10] V.L. Solozhenko, Y. Le Godec, O.O. Kurakevych, C. R. Chim. 9 (2006) 1472–1475.
[11] The sample has been obtained by the arc remelting of amorphous boron in the argon medium.
[12] V.L. Solozhenko, T. Peun, J. Phys. Chem. Solids 58 (1997) 1321–1323.
[13] V.L. Solozhenko, G. Will, F. Elf, Solid State Commun. 96 (1995) 1–3.
[14] A. LeBail, H. Duroy, H.J.L. Fourquet, Mater. Res. Bull. 23 (1988) 447–452.
[15] A.C. Larson, R.B. Von Dreele, General Structure Analysis System (GSAS), Los Alamos National Laboratory Report LAUR, 2000; pp. 86–748.
[16] Y. Wang, J. Fan, M. Trenary, J. Chem. Mater. 5 (1993) 192–198.
[17] A. Kirfel, A. Gupta, G. Will, Acta Crystallogr. B 35 (1979) 1052–1059.
[18] B.F. Decker, J.S. Kasper, Acta Crystallogr. 12 (1959) 503–506.

[19] T.L. Aselage, D.R. Tallant, D. Emin, Phys. Rev. B 56 (1997) 3122–3129.
[20] I. Higashi, M. Kobayashi, J. Bernhard, C. Brodhag, F. Thevenot, in: AIP Conference Proceedings, vol. 231, 1991, pp. 201–204.
[21] K. Ploog, H. Schmidt, E. Amberger, G. Will, K.H. Kobossobutzki, J. Less Common Met. 29 (1972) 161–169.
[22] W. Kraus, G. Nolze, Program PowderCell 2.4, FIMRT, Berlin, 2000.
[23] V.A. Mukhanov, O.O. Kurakevych, V.L. Solozhenko, High Pressure Res. 28 (2008) 531–537.
[24] V.A. Mukhanov, O.O. Kurakevych, V.L. Solozhenko, J. Superhard Mater. 30 (2008) 368–378.